Journal of Alloys and Compounds 509 (2011) 8738–8741

Contents lists available at ScienceDirect

Journal of Alloys and Compounds

journal homepage: www.elsevier.com/locate/jallcom

Vitreous phase coating on glaserite-type alkaline earth silicate blue phosphor $BaCa_2MgSi_2O_8:Eu^{2+}$

Yoshinori Yonesaki*, Qiang Dong, Nur Suhaiza Binti Mohamad, Akira Miura, Takahiro Takei, Junji Yamanaka, Nobuhiro Kumada, Nobukazu Kinomura

Interdisciplinary Graduate School of Medicine and Engineering, University of Yamanashi, Miyamae 7-32, Kofu 400-8511, Japan

ARTICLE INFO

Article history:
Received 10 February 2011
Received in revised form 9 June 2011
Accepted 13 June 2011
Available online 25 June 2011

Keywords:
Amorphous materials
Coating materials
Phosphors
Luminescence

ABSTRACT

A simple solid-state reaction was used to apply a vitreous-phase coating onto Eu^{2+}-doped $BaCa_2MgSi_2O_8$ blue-phosphor particles. The vitreous phase was generated by liquid phase sintering at 1200 °C. The coated phosphor exhibited resistant to an acid dispersant. When a small amount of Al and La was added in raw materials, they were incorporated in the vitreous coating phase.

1. Introduction

In the last few decades, a numerous number of inorganic phosphors have been developed. In particular, Eu^{2+}-activated phosphors have been actively researched because the intense visible emission and color controllability are applicable for various lighting devices. Since Eu^{2+} emission character is largely dependent on the coordination environment, the host material should be carefully chosen for phosphor development. Silicate-based materials are appropriate for the Eu^{2+}-activated phosphors [1–17] since their high structural and thermal stability enable hard usage. In recent years, an alkaline earth orthosilicate $Ba_3MgSi_2O_8:Eu^{2+}$ has attracted much attention because of the intense pure blue emission under UV or VUV excitation. Their luminescence character has been intensively studied by many research groups [1–10]. However, $Ba_3MgSi_2O_8$ has a serious problem of structural instability against UV irradiation [18]. Therefore, design of the related phosphor has been attempted to overcome this problem. In our previous report, we investigated the crystal structure of $M_3MgSi_2O_8:Eu^{2+}$ (M: Ba, Sr, Ca) layered orthosilicates (Fig. 1), and it has been clarified that the instability of $Ba_3MgSi_2O_8$ is caused by the Ba^{2+} ions at layer-embedded B-site [18]. Based on the obtained results, we propose $BaCa_2MgSi_2O_8$ (BCMS), in which the layer-embedded B-site is occupied by Ca^{2+} ions, as an alternative host material [20]. The Ca-substituted compound has been confirmed to be tolerant to UV irradiation. However, in actual usage, phosphor materials are expected to have high chemical durability. In order to improve the durability, encapsulation of individual phosphors has been attempted by sol–gel process of tetraethyl orthosilicate (TEOS) and by heterocoagulation process of colloidal silica [21–26]. In the case of $M_3MgSi_2O_8$ orthosilicates, however, similar vitreous-phase coating can be formed by careful control of synthesis temperature since the $M_3MgSi_2O_8$ contains a typical glass network former SiO_2 as a constituent. In this report, a vitreous phase coating was deposit on BCMS:Eu^{2+} particles by a simple heat treatment process. The chemical durability of the coated BCMS:Eu^{2+} was checked by acid test using hydrochloric solution. The addition of aluminum and phosphorous to the coating was also attempted.

2. Experimental

2.1. Synthesis

Powder samples were prepared from reagent grade $BaCO_3$, $CaCO_3$, magnesium carbonate hydroxide, SiO_2, $(NH_4)_2HPO_4$, Al_2O_3, La_2O_3, Na_2CO_3 and Eu_2O_3. A small amount of NH_4Cl was used as a flux. Stoichiometric amounts of the reagents and the flux were ground and mixed by ball milling with zirconia beads in 2-propanol for 4 h to form $Ba(Ca_{1.98-x}La_xEu_{0.02})Mg(Si_{2-x}Al_x)O_8$ and $Ba(Ca_{1.98-y}Na_yEu_{0.02})Mg(Si_{2-y}P_y)O_8$ (x, y = 0.00–0.05). The mixed reagent powder was heated at 1100 or 1200 °C for 4 h in a flow of 2% H_2–98% N_2 gas with an intermittent re-grinding.

2.2. Characterization

The prepared samples were checked by X-ray powder diffraction (XRD) on a Rigaku RINT-2200HFV diffractometer using CuKα radiation. Diffraction data were collected at intervals of 0.05° from 10° to 120° 2θ at room temperature. Room-temperature infrared (IR) transmission spectra were measured by a KBr pellet method with a JASCO FT/IR-4100 spectrometer. The morphology of the sample particles was observed by field-emission scanning electron microscope (FE-SEM) using

* Corresponding author. Tel.: +81 55 220 8723; fax: +81 55 254 3035.
E-mail address: yonesaki@yamanashi.ac.jp (Y. Yonesaki).

0925-8388/$ – see front matter © 2011 Elsevier B.V. All rights reserved.
doi:10.1016/j.jallcom.2011.06.042

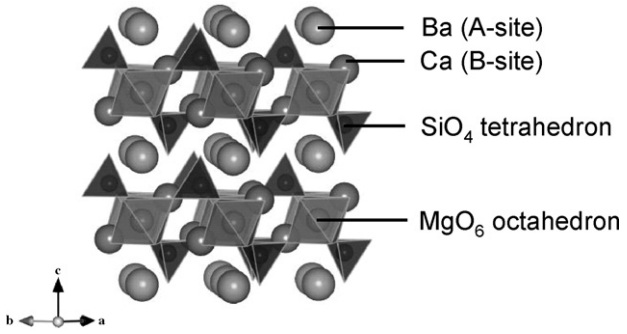

Fig. 1. Crystal structure of $BaCa_2MgSi_2O_8$ (drawn with VESTA [19]).

a JEOL Ltd. JSM-6500F. For the prepared samples, emission spectra were measured at room temperature using a JASCO corporation FP-6500 spectrofluorometer with a xenon discharge lamp used as excitation source. Excitation wavelength was 254 nm.

2.3. Acid test

The chemical durability of the prepared samples was checked by a HCl acid test. The acid test consisted of placing 0.5 g of a sample in the bottom of a beaker and filling with 50 mL of HCl solution of pH = 4. Two days after, the suspension was filtered and dried, and then, the remaining phosphor powder was weighed. Chemical durability was evaluated from the weight reduction after the immersion.

3. Results

3.1. XRD analysis

Fig. 2 shows the XRD patterns for the prepared samples. Indices are assigned to the diffraction peaks of BCMS phase. The obtained patterns agree well with the previous data [20]. When heated at 1100 °C (Fig. 2(a)), the obtained samples contain Al, La-derived impurities, depending on the additive amount. As for the BCMS phases in the products, no significant peak shift is observed, irrespective of the additive amount. These results indicate that BCMS structure was not affected by Al, La-addition. In the case of 1200 °C synthesis, the Al, La-derived impurities disappeared (Fig. 2(b)). Instead, as Al, La-additives increase, the diffraction peaks of BCMS slightly shift to higher 2θ, which can be clearly seen in a high 2θ region (inset of Fig. 2(b)). Namely, Al, La-addition induced the shrinkage of the BCMS unit cell in the case of 1200 °C synthesis.

On the other hand, when P and Na are involved in the raw materials, $MgSiO_3$ appears as an impurity phase (Fig. 2(c) and (d)). The amount of $MgSiO_3$ monotonically increases with an increase in P, Na-additives. No significant peak shift is confirmed for the BCMS phase, regardless of synthesis temperature. From these results, phosphorus addition leads to impurity generation and has little influence on BCMS structure.

3.2. IR spectroscopy

Fig. 3 shows the IR absorption spectra of the samples. Intense absorption peaks appear at about 895, 1020, and 520 cm^{-1} for all the samples. Generally, absorption peaks at such high wavenumbers are attributed to internal vibrations of certain atomic groups. In the present case, they are derived from three of the four normal modes of SiO_4 vibration: symmetric stretching vibrations (ν_1), asymmetric stretching vibrations (ν_3) and asymmetric bending vibrations (ν_4), respectively. These spectra reveal that IR absorption character is mainly influenced by synthesis temperature, not by additives. It can be seen that Al, La- or P, Na-addition has little influence on SiO_4 internal vibrations. Instead, as synthesis temperature increases, SiO_4-derived absorption peaks become broader (Fig. 3(b)), compared to the case of 1100 °C synthesis (Fig. 3(a)). This broadening reflects that high temperature process generated many types of SiO_4 tetrahedra with different vibrational frequencies. However, the broadening is not so obvious for the P, Na-added sample.

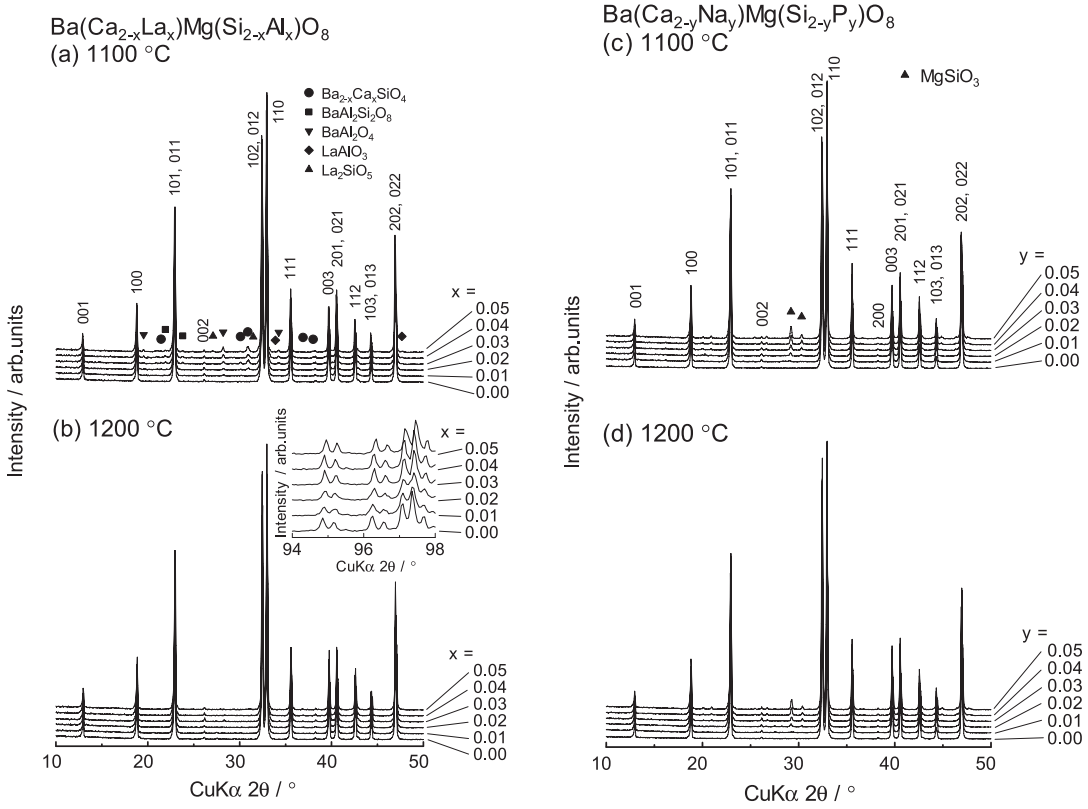

Fig. 2. X-ray powder diffraction patterns for $Ba(Ca_{1.98-x}La_xEu_{0.02})Mg(Si_{2-x}Al_x)O_8$ (synthesized at 1100 °C (a) and 1200 °C (b)) and $Ba(Ca_{1.98-y}Na_yEu_{0.02})Mg(Si_{2-y}P_y)O_8$ (synthesized at 1100 °C (c) and 1200 °C (d)).

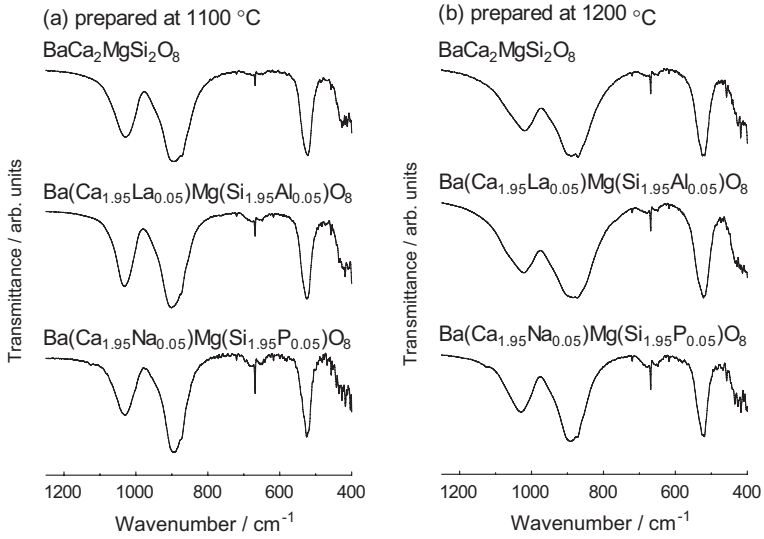

Fig. 3. IR absorption spectra for the samples synthesized at 1100 °C (a) and 1200 °C (b).

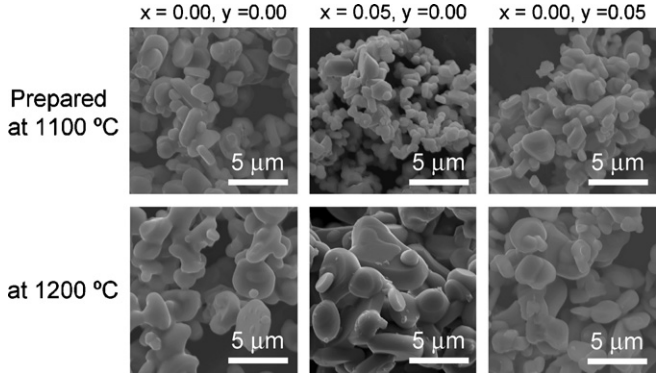

Fig. 4. SEM images of $Ba(Ca_{1.98-x}La_xEu_{0.02})Mg(Si_{2-x}Al_x)O_8$ and $Ba(Ca_{1.98-y}Na_yEu_{0.02})Mg(Si_{2-y}P_y)O_8$.

3.3. SEM images

Fig. 4 shows SEM images of the samples. In the case of 1100 °C synthesis, all the products show similar morphology. They involve grains about 1 μm in size. Each particle is clearly separated. It can be also observed that a part of fully grown particles show hexagonal shape, which reflects the crystal system of BCMS. On the other hand, in the case of 1200 °C synthesis, morphology changes. For the pure and Al-added samples (Fig. 4, $y = 0.00$), particles with the size of 3–4 μm aggregate through a meniscus (neck between particles) and have rounded shape. However, when phosphorus ions are added (Fig. 4, $y = 0.05$), each particle moderately maintains its idiomorphic shape and is fully separated.

3.4. Emission spectra

All the Eu-doped samples exhibited blue emissions under 254-nm excitation. Fig. 5 shows emission spectra for the samples. The broad emission peak originates in 5d–4f electron transition in divalent europium ions. Each peak has a shoulder at about 450 nm, which comes from Eu^{2+} ions at two crystallographically different sites [20]. In the case of 1100 °C synthesis, Al, La- or P, Na-addition hardly interferes with Eu^{2+}-emission character (peak position, profile and intensity do not change by the additives). However, 1200 °C-synthesized Al, La-added samples exhibit a lowering in emission intensity (Fig. 5(b)). The low emission intensity is probably caused by defects or a low relative amount of BCMS phase in the product.

Table 1
Weight of the remaining sample after two days of HCl acid test.

Sample	Weight (%)
BCMS synthesized at 1100 °C	86
BCMS synthesized at 1200 °C	98
$Ba(Ca_{1.95}La_{0.05})Mg(Si_{1.95}Al_{0.05})O_8$ synthesized at 1200 °C	96

3.5. Acid test

Table 1 shows the results of the acid test. Only the 1100 °C-synthesized sample showed clear weight loss from dissolution. However, the sample dissolution was suppressed by 1200 °C synthesis. After the acid test, the samples still exhibited the Eu^{2+}-derived blue emission. Spectral changes were not confirmed. Their XRD patterns assured that the Eu^{2+}-doped samples maintained the BCMS structure.

4. Discussion

4.1. Low temperature (1100 °C) synthesis

The pure BCMS product involved fully separated particles (Fig. 4, $x = 0.00$, $y = 0.00$). A part of them had idiomorphic hexagonal shape, which assured the high crystallinity of the particles. As shown in XRD results (Fig. 2(a)), Al-addition had little influence on the BCMS structure. IR spectra for the pure and Al-added (Fig. 3(a)) also support the structural similarity of the BCMS phase in the products. Al and La were involved in impurities, such as $BaAl_2Si_2O_8$ and $LaAlO_3$. These results suggest that Al and La were excluded from the BCMS crystal structure. In the case of P, Na-addition, P-free $MgSiO_3$ appeared as an impurity phase (Fig. 2(c) and (d)). Probably, phosphorus vaporization caused non-stoichiometry, leading to the P-free impurity. The phosphorus vaporization was confirmed by energy-dispersive X-ray spectroscopy of the products.

4.2. High temperature (1200 °C) synthesis

From the XRD patterns of the pure and Al-added samples (Fig. 2(b)), only BCMS phase was identified. However, it can be concluded that Al or La was not involved in the BCMS phase because, with aluminum amount increasing, the BCMS unit cell shrunk (inset of Fig. 2(b)). If Al occupied Si site (or La occupied Ca site), unit cell would be expanded because of the large ionic radius [27]. In the present case, the opposite is true. Al and La might be involved in

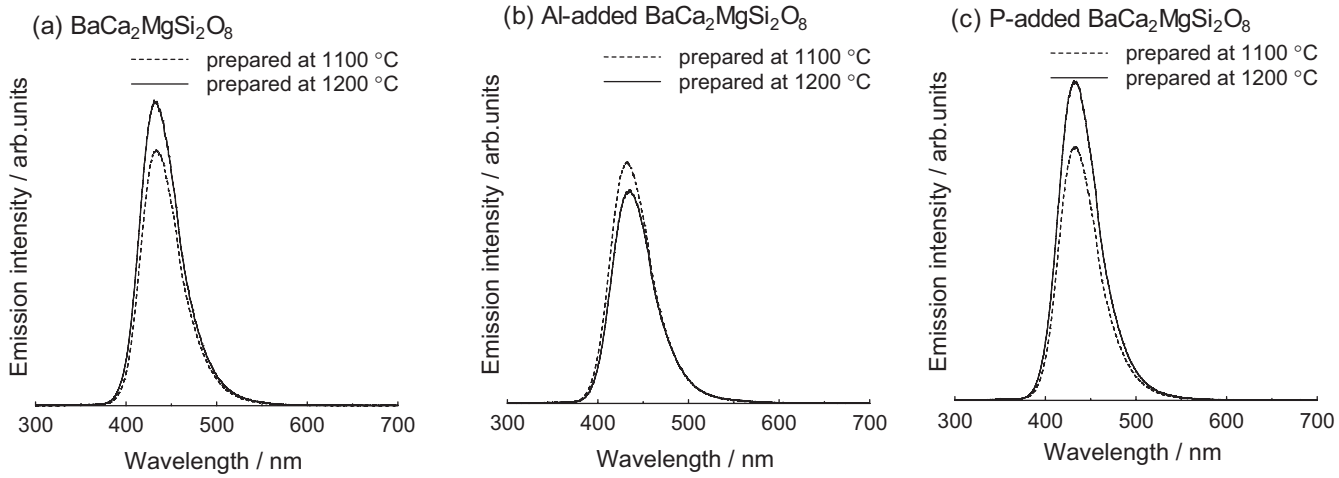

Fig. 5. Emission spectra for $Ba(Ca_{1.98}Eu_{0.02})MgSi_2O_8$ (a), $Ba(Ca_{1.93}La_{0.05}Eu_{0.02})Mg(Si_{1.95}Al_{0.05})O_8$ (b) and $Ba(Ca_{1.93}Na_{0.05}Eu_{0.02})Mg(Si_{1.95}P_{0.05})O_8$ (c). Excitation wavelength was 254 nm.

a vitreous phase which could not be detected by XRD. Imaoka et al. have closely investigated the vitreous-phase formation range of MO–MgO–SiO_2 systems [28]. According to their results, the chemical composition of $M_3MgSi_2O_8$ (M: Ba, Sr, Ca) is located in the border between vitreous-phase formation and crystallization. Lara et al. reported similar results [29]. Taking their results into account, it is believed that a vitreous phase of BCMS composition was generated during 1200 °C process. In a vitreous silicate, there are various types of SiO_4 tetrahedra in the random network. The peak broadening in IR absorption spectra (Fig. 3(b)) assures a variety of SiO_4 tetrahedron. The particle growth and the rounded form in SEM images also support the presence of liquid phase under the 1200 °C condition. The particle growth with meniscus behavior (Fig. 4) originated in liquid phase sintering. Probably, in cooling, the melt involving SiO_2, a typical glass network former, and Al_2O_3, an intermediate, formed a vitreous phase together with some constituents, such as Ba, Ca and La. The observed unit cell shrinkage for BCMS (Fig. 2(b)) probably came from defects induced by non-stoichiometry accompanied by the vitreous-phase formation. From these results, we can conclude that a vitreous phase coating was obtained for BCMS:Eu^{2+} phosphors by a simple solid state reaction at 1200 °C. Although such a meniscus behavior was not confirmed for the P, Na-added samples, it was probably due to that SiO_2 component was consumed for $MgSiO_3$ (Fig. 2(d)).

4.3. Usefulness of vitreous phase coating on BCMS:Eu^{2+} phosphor

The results of acid test clearly show that the high temperature synthesis has improved the chemical durability of the BCMS:Eu^{2+} phosphor. It is considered that the high chemical durability was achieved by the vitreous phase coating, as reported for other coated phosphors [21–26]. In the present study, added aluminum did not show an effective result. However, it has been reported that aluminosilicate glass has high values of elastic moduli and a high resistance to chemical corrosion because aluminum decreases non-bridging oxygen in the random network [30]. Therefore, the Al-containing vitreous coating obtained in this study is expected to be more durable against thermal shock. In order to demonstrate the mechanical strength, further research is required.

5. Conclusions

A vitreous-phase coated $BaCa_2MgSi_2O_8$:Eu^{2+} phosphor was prepared by a simple solid state reaction at 1200 °C. The coating phase enhanced acid durability of the phosphor. XRD analyses reveal that Al, La-additives were incorporated in the coating phase. The coating phase modified by Al and La potentially improves the chemical and mechanical durability of the coated phosphor particles.

Acknowledgment

The author Y. Yonesaki is indebted to the financial support for the present research by Nippon Sheet Glass Foundation for Materials Science and Engineering.

References

[1] T.L. Barry, J. Electrochem. Soc. 115 (1968) 733–738.
[2] J.S. Kim, P.E. Jeon, J.C. Choi, H.L. Park, Appl. Phys. Lett. 84 (2004) 2931–2933.
[3] J.S. Kim, J.Y. Kang, P.E. Jeon, J.C. Choi, H.L. Park, T.W. Kim, Jpn. J. Appl. Phys. 43 (2004) 989–992.
[4] J.S. Kim, K.T. Lim, Y.S. Jeong, P.E. Jeon, J.C. Choi, H.L. Park, Solid State Commun. 135 (2005) 21–24.
[5] H.K. Jung, K.S. Seo, Opt. Mater. 28 (2006) 602–605.
[6] J.S. Kim, A.K. Kwon, Y.H. Park, J.C. Choi, H.L. Park, G.C. Kim, J. Lumin. 122–123 (2007) 583–586.
[7] Y. Umetsu, S. Okamoto, H. Yamamoto, J. Electrochem. Soc. 155 (2008) J193–J197.
[8] L. Ma, D.J. Wang, Z.Y. Mao, Q.F. Lu, Z.H. Yuan, Appl. Phys. Lett. 93 (2008) 144101.
[9] L. Ma, D.J. Wang, H.M. Zhang, T.C. Gu, Z.H. Yuan, Electrochem. Solid State Lett. 11 (2008) E1–E4.
[10] D.J. Wang, L.Y. Liu, Electrochem. Solid State Lett. 12 (2009) H179–H181.
[11] W.B. Im, Y.I. Kim, H.S. Yoo, D.Y. Jeon, Inorg. Chem. 48 (2009) 557–564.
[12] W.H. Hsu, M.H. Sheng, M.S. Tsai, J. Alloys Compd. 467 (2009) 491–495.
[13] C.H. Hsu, R. Jagannatan, C.H. Lu, Mater. Sci. Eng. B 167 (2010) 137–141.
[14] X. Zhang, X. Tang, J. Zhang, M. Gong, J. Lumin. 130 (2010) 2288–2292.
[15] X. Zhang, X. Tang, J. Zhang, H. Wang, J. Shi, M. Gong, Powder Technol. 204 (2010) 263–267.
[16] C. Fu, Y. Hu, Y. Wang, H. Wu, X. Wang, J. Alloys Compd. 502 (2010) 423–428.
[17] Y. Li, Y. Wang, X. Xu, O. Yu, F. Zhang, J. Electrochem. Soc. 157 (2010) J39–J43.
[18] Y. Yonesaki, T. Takei, N. Kumada, N. Kinomura, J. Solid State Chem. 182 (2009) 547–554.
[19] K. Momma, F. Izumi, J. Appl. Crystallogr. 41 (2008) 653–658.
[20] Y. Yonesaki, T. Takei, N. Kumada, N. Kinomura, J. Lumin. 128 (2008) 1507–1514.
[21] G.L. Messing, S.C. Zhang, G.V. Jayanthi, J. Am. Ceram. Soc. 76 (1993) 2707–2726.
[22] L. Nikolic, L. Radonjic, Ceram. Int. 24 (1998) 547–552.
[23] Y. Azuma, K. Nogami, N. Ohshima, J. Ceram. Soc. Jpn. 100 (1992) 646–651.
[24] J.H. Jean, S.M. Yang, J. Am. Ceram. Soc. 83 (2000) 1928–1934.
[25] G.R. Villalobos, S.S. Bayya, J.S. Sanghera, R.E. Miklos, F. Kung, I.D. Aggarwal, J. Am. Ceram. Soc. 85 (2002) 2128–2130.
[26] Y.R. Do, D.H. Park, H.G. Yang, W. Park, B.K. Wagner, K. Yasuda, C.J. Summers, J. Electrochem. Soc. 148 (2001) G548–G551.
[27] R.D. Shannon, Acta Crystallogr. A32 (1976) 751–767.
[28] M. Imaoka, T. Yamazaki, J. Ceram. Assoc. Jpn. 71 (1963) 215–223.
[29] C. Lara, M.J. Pascual, A. Duran, J. Non-Cryst. Solids 348 (2004) 149–155.
[30] A.K. Varshneya, Fundamentals of Inorganic Glasses, Academic Press, INC., New York, 1994.